

EXPERIMENTAL STUDY OF STIBNITE SOLUBILITY IN AQUEOUS SULFIDE SOLUTIONS FROM 25 TO 90°C

Nellie J. Olsen^{1,2}, Bruce W. Mountain¹ and Terry M. Seward²

¹ GNS Science, Wairakei Research Centre, Private Bag 2000, Taupo 3352, New Zealand

² SGees, Victoria University of Wellington, PO Box 600, Wellington 6140, New Zealand

n.olsen@gns.cri.nz

Keywords: Antimony, stibnite, geothermal scaling, geochemical modeling

ABSTRACT

Modelling antimony transport in hydrothermal systems and developing mitigation procedures for stibnite (Sb_2S_3) scaling in geothermal power stations, such as those at the Ngawha and Rotokawa geothermal systems, requires precise thermodynamic data to determine stibnite solubility under different physicochemical conditions. Specifically, accurate modelling requires knowledge of the dependence of stibnite solubility and complexation on pH, sulfide concentration and temperature. However, there is uncertainty in the stability and stoichiometry of antimony(III) sulfide/ hydrosulfide complexes at 25°C and higher temperatures that prevents detailed modelling of the transport and precipitation chemistry of antimony in aqueous sulphide media at elevated temperatures.

We have conducted solubility experiments with natural stibnite in a flow-through apparatus to determine the solubility of stibnite in aqueous sulfide solutions from pH 6.0 to 12.5 and sulfide concentrations from 0.002 to 0.2 mS_{total} at 25°C. The apparatus also allows measurement of stibnite solubility at elevated temperatures up to 90°C. These experiments are underway.

Our experimental results are similar to the solubilities found at 25°C by Krupp (1988). He concluded that $H_xSb_2S_4^{x-2}$ species are dominant between pH 3 to 12, but other authors have suggested $H_xSb_2S_2O_2^{x-2}$ and $H_xSbS_3^{x-3}$ species (Wood, 1989; Tossell, 1994). We note that for arsenic, H_3AsS_3 is apparently the dominant thioarsenite stoichiometry (Bostick et al., 2005; Beak et al., 2008; Zakaznova-Herzog and Seward, 2012). At 90°C, our solubilities are similar to solubilities extrapolated to higher pH from Krupp (1988). Our measurements will provide a complete set of stibnite solubility measurements between 25 and 90°C in reduced, sulfide-containing fluids and permit a new evaluation of the stoichiometry and stability of thioantimonite species at these conditions.

1. INTRODUCTION

1.1 Modeling antimony (Sb) in hydrothermal fluids

Stibnite (Sb_2S_3) is the most common antimony mineral, and its solubility is a primary control on the concentration of antimony hydrothermal fluids. The ability to predict changes in stibnite solubility and aqueous antimony complexation in response to changes in pH, temperature and aqueous sulphide content is necessary in modelling antimony behaviour during hydrothermal ore deposition and in other environments characterised by high-temperature, reducing, sulfide-containing fluids, including within geothermal power generation systems.

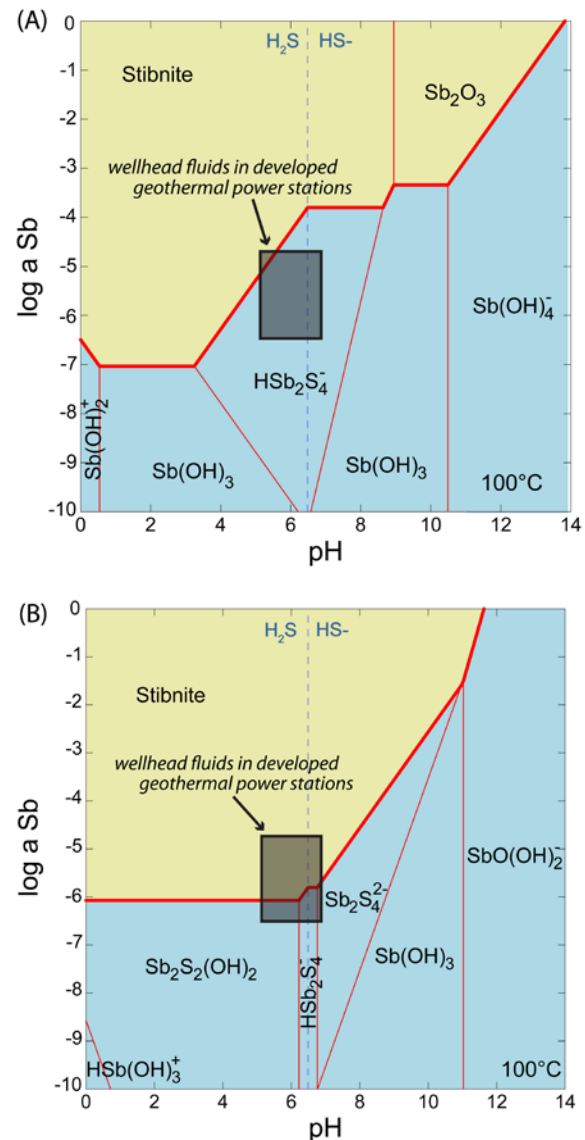


Figure 1: Speciation diagrams for antimony using different thermodynamic databases. Speciation diagrams for antimony at 100°C in the presence of 0.0005 mol/kg total reduced sulfur ($H_2S_{(aq)} + HS^-$) using: (A), the thermo.comV8R6.data database provided with Geochemist's Workbench Standard® 9.0 and in which antimony data is based primary on Spycher and Reed (1989) and, (B), data calculated by the authors from Krupp (1988), Suleimenov and Seward (1997), Zakaznova-Herzog and Seward (2006) and Wilson et al. (2007). Wellhead conditions are based upon analyses for systems in Italy, New Zealand and El Salvador reported in Raymond et al. (2005), Ward et al. (2006), Wilson et al. (2007) and Morteani et al. (2011).

In reducing hydrothermal solutions, antimony occurs in the trivalent oxidation state (Sb^{+3} , antimonite) and may form a variety of aqueous complexes with hydroxide (OH^-) and/or sulfide (HS^-) ligands. Modelling antimony chemistry relies on accurate thermodynamic data for these thio- and oxythioantimonite complexes. Antimony complexation in the $\text{Sb(III)}\text{-HS-OH-H}$ system has been studied using a variety of solubility (Arnston et al., 1966; Kolpakova, 1982; Krupp 1988; Akinifiyev et al., 1994; Belevanstev et al., 1998), spectroscopic (Wood, 1989; Gushchina et al., 2000; Mosselmans et al., 2000) and theoretical methods (Tossell, 1994). Krupp (1988) concluded that $\text{H}_x\text{Sb}_2\text{S}_4^{x-2}$ species are dominant between $\text{pH} = 3$ to 12 at temperatures up to 100°C when aqueous sulfide is 0.01 mol/kg, with the anion $\text{HSb}_2\text{S}_4^{-1}$ being the most abundant in the near pH region. Other authors have suggested $\text{H}_x\text{Sb}_2\text{S}_2\text{O}_2^{x-2}$ and $\text{H}_x\text{SbS}_3^{x-3}$ species among others (Wood, 1989; Tossell, 1994).

Compilations of stibnite thermodynamic data have been done by several authors to produce thermodynamic databases for modelling antimony chemistry (e.g. Spycher and Reed, 1989; Obolensky et al., 2007). Figure 1 contains two plots that are examples of activity diagrams for the same geochemical conditions (100°C and 0.0005 mol/kg H_2S) produced by two different compilations of antimony thermodynamic data. Several of the same aqueous species occur within both diagrams, but the solubility of stibnite at pH 7 varies by about two orders of magnitude between the two models of antimony speciation. Figure 1 also includes a region between $\text{pH} = 5.5$ to 7 and antimony concentrations from 10^{-6} to $10^{-4.8}$ mol/kg Sb that is inclusive of conditions observed in geothermal fluids from production wellhead samples in several geothermal systems, as discussed further in the next section. Depending upon which database is used, the fluids are either primarily oversaturated or primarily under saturated with respect to stibnite. Comparing the models presented in Figure 1 it is clear that a critical re-examination of the thermodynamic data for antimony speciation is needed.

1.2 Antimony scaling in geothermal power stations

Stibnite and antimony-rich sulphide scaling within pipelines in geothermal power stations has been observed in a number of geothermal systems, including in Italy, El Salvador and New Zealand (Cappetti et al., 1995; Raymond et al., 2005; Wilson et al., 2007; Morteani et al. 2011). In New Zealand, stibnite scaling has been observed at the Ngawha and Rotokawa geothermal stations, most abundantly in the mixed brine-condensate heat exchangers. Based upon thermodynamic modelling, the precipitation of stibnite scale in Rotokawa was attributed to a pH decrease while at Ngawha the temperature decrease was considered more important (Wilson et al. 2007). However, the data used considered a very limited number of thioantimonite species and have not been updated to include recent data for antimonous acid (Sb(OH)); Zakaznova-Herzog and Seward 2006).

2. EXPERIMENTAL APPROACH

We are conducting solubility experiments with natural stibnite in the flow-through apparatus shown in Figure 2. This apparatus consists of a glass flask in which a deoxygenated $\text{NaOH-H}_2\text{S}$ solution was prepared with a given pH and sulfide content. The pH was controlled via addition of varying amounts of sodium hydroxide and the sulfide concentration was controlled by varying the $\text{H}_2\text{S}_{(g)}$ content of the $\text{H}_2\text{S}/\text{N}_2$ gas mixture that was bubbled through the solution during preparation. This solution was then pumped through two PEEK plastic columns containing crushed and cleaned stibnite. The solution was collected in a syringe and the pH, sulfide content and antimony concentration were measured in the effluent.

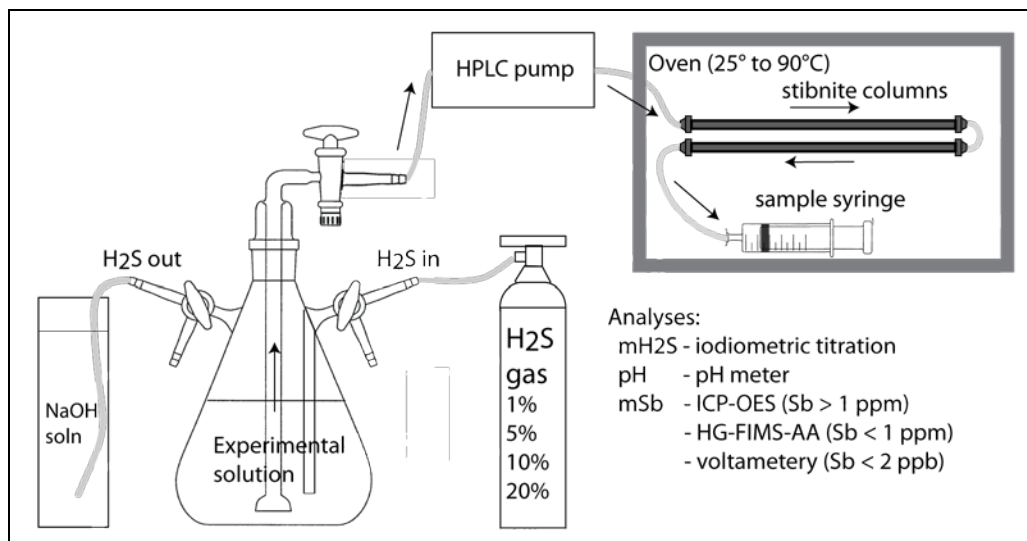
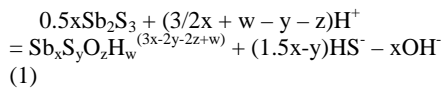


Figure 2: Diagram of experimental apparatus for flow through solubility experiments. $\text{NaOH-H}_2\text{S}$ solutions are prepared by de-oxygenation of distilled water and then bubbling a $\text{N}_2/\text{H}_2\text{S}$ gas mixture through the solution. A HPLC pump moves the experimental solution through two columns containing crushed stibnite and into a collection syringe. Samples are taken periodically when there is enough effluent for analyses of total reduced sulphur ($\text{S}_{(\text{total})}$), pH and total antimony.

These stibnite solubility experiments produce the equilibrium antimony aqueous concentration at a given pH and S_{total} ($= H_2S + HS^-$). Conducting experiments at variable pH and S_{total} produces stibnite solubility curves, and the complexes present can be determined by fitting possible aqueous complexes to the experimentally measured curves. For example, stibnite solubility in the presence of any aqueous hydrosulfide antimony(III) complex in the pH region dominated by HS^- can be described by the following general equation:



in which the variables x, y, z and w indicate the stoichiometry of the aqueous antimony complex ($Sb_xS_yO_zH_w$). The partial derivative of equation (1) with respect to pH

$$\delta Sb_{\text{total}}/\delta pH = 2z + y - w - 1.5x \quad (2)$$

or HS^- ,

$$\delta Sb_{\text{total}}/\delta S_{\text{total}} = y - 1.5x \quad (3)$$

gives the slope of a stibnite solubility curve with respect to pH or H_2S for any given antimony complex. The $\delta Sb_{\text{total}}/\delta pH$ and $\delta Sb_{\text{total}}/\delta S_{\text{total}}$ pairs for a selection of possible complex stoichiometries are given in Figure 4. The stoichiometries included are those hypothesized for the $Sb(\text{III})$ -HS-OH-H system by previous authors (Arnston et al., 1966; Shestikov and Demina, 1971; Krupp, 1988; Wood, 1989; Tossell, 1994; Zakaznova-Herzog and Seward, 2006).

2.2 Determination of equilibrium

It is critical that equilibrium is reached in solubility studies. Equilibrium is determined by measuring the Sb concentration at different flow rates as shown in Figure 4. When the aqueous antimony concentration reaches a maximum value and does not increase with decrease flow rate, experiments are considered to have reached equilibrium. The flow rate at which the experimental system reaches equilibrium is a greater in experiments with a higher pH and/or temperature and so different experiments have been conducted at different flow rates.

3. RESULTS

We have conducted experiments in aqueous sulfide solutions from pH = 6.0 to 12.5 and sulfide contents from 0.002 to 0.2 mS_{total} at 25°C, and, at ~ 90°C, from pH = 8 to 10.5 at sulfide contents from 0.002 to 0.009 mS_{total}. The preliminary room temperature and 90°C results are presented and compared to the previous data of Krupp (1988) in Figures 5 and 6, respectively.

Our experimental results are similar to the solubilities found at 25°C by Krupp (1988) at pH = 11 – 12 but our higher measured stibnite solubilities pH ≈ 8 suggest that Krupp (1988) may have under estimated stibnite solubility at some experimental conditions.

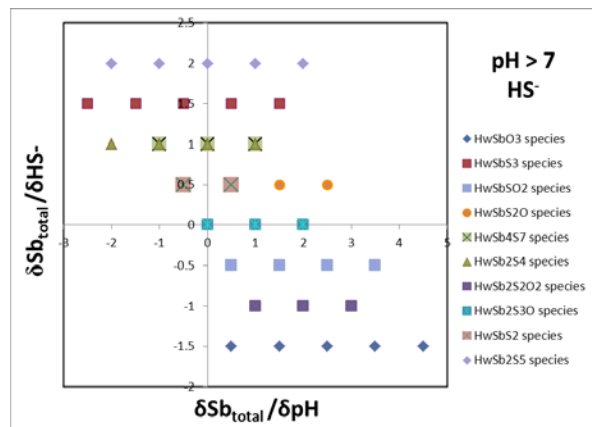


Figure 3: Ideal slopes of stibnite solubility curve ($\delta Sb_{\text{total}}/\delta pH$ and $\delta Sb_{\text{total}}/\delta S_{\text{total}}$) for selected complexes. Slopes are calculated using equations 2 and 3. Vertical position is determined by a species' Sb:S:O ratio and horizontal position by the degree of protonation (i.e. the variable w in equations 1 and 2).

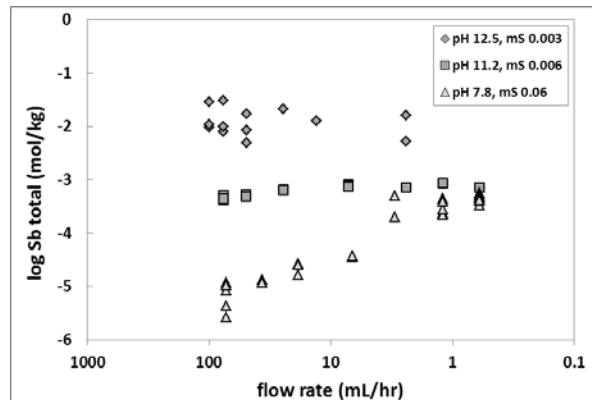


Figure 4: Flow rate versus solubility curves for selected experimental conditions.

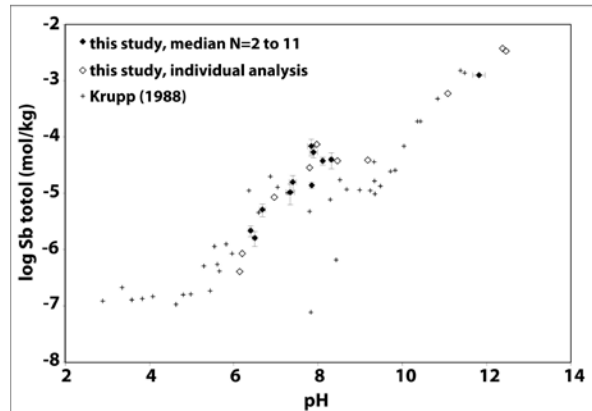


Figure 5: Experimental solubility curve projected to $S_{\text{total}} = 0.01$. Filled diamonds indicate medians of multiple analyses, and error bars are 2*standard deviations for both antimony and pH. Open diamonds indicate single analyses. Crosses are experimental data from Krupp (1988). All data has been projected from the measured S_{total} to $S_{\text{total}} = 0.01$ mol/kg using the aqueous species suggested by Krupp (1988).

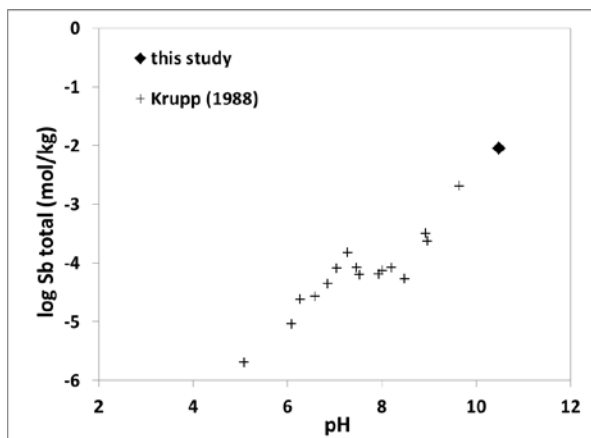


Figure 6: Comparison of preliminary results at 90°C and data from Krupp (1988). Comparison of data from an 87°C experiment at pH = 10.5 and $S_{\text{total}} = 0.0086$ mol/kg with data from Krupp (1988) at similar temperature (90°C) and total sulfur content (0.0076 to 0.0096 mol/kg). Error bars for our data are 2*standard deviations for both antimony and pH and are smaller than the symbol for the experiment plotted.

As shown in Figure 6 for a selected experiment, at $\sim 90^\circ\text{C}$, our solubilities are similar to solubilities extrapolated to high pH from 90°C experiments conducted at the similar sulphide contents by Krupp (1988). Further experiments at 25 and 90°C are on-going.

4. CONCLUSIONS

Geochemical modelling of antimony behaviour in hydrothermal fluids is currently limited by the quality and completeness of the thermodynamic available, particularly for thioantimonite and possibly for oxythioantimonite species. Some of the most readily available thermodynamic databases are not up-to-date, and the speciation models they produce vary widely (Figure 1). The most complete stibnite solubility study (Krupp, 1988) extends from pH = 3 to 12 but the data is especially scattered in the pH range from pH = 6 to 9, which corresponds to the range of most natural geothermal fluids. Additionally, thermodynamic data from Krupp (1988) and others are limited at higher temperatures.

Our stibnite solubility experiments conducted using a flow-through apparatus at 25°C produce preliminary results that suggest that the solubilities measured by Krupp (1988) are comparable (albeit somewhat scattered) but that speciation may need to be re-evaluated.

As with antimonite, studies of arsenite (As^{3+}) complexation in sulfide-containing fluids have produced a wide range of possible stoichiometries for thioarsenites (Zakaznova-Herzog and Seward, 2012 and references therein). However, some recent studies have favoured H_3AsS_3 as the dominant thioarsenite stoichiometry (Bostick et al., 2005; Beak et al., 2008; Zakaznova-Herzog and Seward, 2012). Having quality thermodynamic data for thioantimonites and knowing whether thioantimonite speciation is similar to or different from thioarsenite speciation would be extremely useful for investigating and comparing these elements' behaviour in natural hydrothermal systems.

ACKNOWLEDGEMENTS

The authors would like to thank the staff of the GNS Science Analytical Laboratory and Marc-Alban Millet formerly of SGEES for assistance with analyses.

REFERENCES

Akinifiyev, N.N., Zotov, A.V., Shikina, N.D.: Experimental Studies and Self-Consistent Thermodynamic Data in the Sb(III)-S(II)-O-H System. *Geochemistry International* 31 pp. 27-40. (1994).

Arnston, R.H., Dickson, F.W., Tunnel, G.: Stibnite (Sb_2S_3) solubility in sodium sulfide solution. *Science* 153, pp. 1673-1674. (1966).

Beak, D.G., Wilkin, R.T., Ford, R.G., Kelly, S.D.: Examination of arsenic speciation in sulfidic solutions using X-ray absorption spectroscopy. *Environ. Sci. Technol.* 42, pp. 1643-1650. (2008).

Belevantsev, V.I., Gushchina, L.V., Obolensky, A.A.: Solubility of Stibnite, $\text{Sb}_2\text{S}_3(\text{cr})$: A Revision of Proposed Interpretations and Refinements. *Geochemistry International* 36, pp. 58-64. (1998).

Bostick, B.C., Fendorf, S. and Brown, Jr. G.E.: In situ analysis of thioarsenite complexes in neutral to alkaline arsenic sulphide solutions. *Mineral. Mag.* 69, pp. 781-795. (2005).

Cappetti, G., D'Olimpio, P., Sabatelli, F., Tarquini, B.: Inhibition of Antimony Sulphide Scale by Chemical Additives: Laboratory and Field Test Results. *Proceedings 1995 World Geothermal Congress*, Florence, Italy, May 18-31, 1995, 2503-2507.

Gushchina, L.V., Borovikov, A.A., Shebanin, A.P.: Formation of Antimony (III) Complexes in Alkali Sulfide Solutions at High Temperatures: An Experimental Raman Spectroscopic Study. *Geochemistry International* 38, pp. 510-513. (2000).

Kolpakova, N.N.: Laboratory and field studies of ionic equilibria in the $\text{Sb}_2\text{S}_3\text{-H}_2\text{O}\text{-H}_2\text{S}$ system. Trans. from *Geokhimiya* 1, pp. 47-55. (1982).

Krupp, R.E.: Solubility of stibnite in hydrogen sulfide solutions, speciation, and equilibrium constants, from 25 to 350°C. *Geochim. et Cosmochim. Acta* 52, pp. 3005-3015. (1988).

Morteani, G., Ruggieri, G., Möller, P., Preinfalk, C.: Geothermal mineralized scales in the pipe system of the geothermal Piancastagnaio power plant (Mt. Amiata geothermal area): a key to understand the stibnite, cinnabarite and gold mineralization of Tuscany (central Italy). *Miner. Deposita* 45, pp. 197-210. (2011).

Mosselmans, J.F.W., Helz, G.R., Patrick, R.A.D., Charnock, J.M., Vaughan, D.J.: A study of Sb in bisulfide solutions by X-ray absorption spectroscopy. *Applied Geochemistry* 15, pp. 879-889. (2000).

Obolensky, A., Gushchina, L., Borisenko, A., Borovikov, A., Pavlova, G.: Antimony in hydrothermal processes: solubility, conditions of transfer, and metal-bearing capacity of solutions. *Russian Geology and Geophysics* 48, pp. 992-1001. (2007).

Raymond, J., Williams-Jones, A.E., Clark, J.R.: Mineralization associated with scale and altered rock and pipe fragments from the Berlín geothermal field, El Salvador; implications for metal transport in natural systems. *Journal of Volcanology and Geothermal Research* 145, pp. 81-96. (2005).

Shestitko, V.S. and Demina, O.P.: Potentiometric determination of the composition of the sulphide anions of antimony. *Russian Journal Inorganic Chemistry* 20, pp. 1679-1680. (1971).

Spycher, N.F. and Reed, M.H.: As(III) and Sb(III) sulfide complexes: An evaluation of stoichiometry and stability from existing experimental data. *Geochim. et Cosmochim. Acta* 53, pp. 2185-2194. (1989).

Suleimenov, O.M. and Seward, T.M.: A spectroscopic study of hydrogen sulphide ionization in aqueous solutions to 250°C. *Geochim. et Cosmochim. Acta* 61, pp. 5187-5198. (1997).

Tossell, J.A.: The speciation of antimony in sulfidic solutions: A theoretical study. *Geochim. et Cosmochim. Acta* 58, pp. 5093-5104. (1994).

Ward, K.T., Brown, K.L., Webster-Brown, J.: Mineral Precipitation in the Rotokawa Geothermal Power Station, New Zealand. Proc. 28th New Zealand Geothermal Workshop, Auckland, New Zealand. pp. (2006).

Wilson, N., Webster-Brown, J., Brown, K.L.: Controls on stibnite precipitation at two New Zealand geothermal power stations. *Geothermics* 36, pp. 330-347. (2007).

Wood, S.A.: Raman spectroscopic determination of the speciation of ore metals in hydrothermal solutions: 1. Speciation of antimony in alkaline sulfide solutions at 25°C. *Geochim. et Cosmochim. Acta* 53, pp. 237-244. (1989).

Zakaznova-Herzog, V.P. and Seward, T.M.: Antimonous acid protonation/deprotonation equilibria in hydrothermal solutions to 300°C. *Geochim. et Cosmochim. Acta* 70, pp. 2298-2310. (2006).

Zakaznova-Herzog, V.P. and Seward, T.M.: A spectroscopic study of the formation and deprotonation of thioarsenite species in aqueous solution at 22°C. *Geochim. et Cosmochim. Acta* 83, pp. 48-60. (2012).